

ACTIVITATEA ANTIBACTERIANĂ A NANOPARTICULELOR DE TiO₂ DOPATE CU Se SINTETIZATE LA TEMPERATURĂ JOASĂ

ANTIBACTERIAL ACTIVITY OF Se DOPED TiO₂ NANOPARTICLES SYNTHESIZED AT LOW TEMPERATURE

MAHAMASUHAIMI MASAE^{1*}, LEK SIKONG², WITTHAYA SRIRIKUN¹

¹Department of Industrial Engineering, Faculty of Engineering, Rajamangala University of Technology Srivijaya, Songkhla, Thailand

²Department of Mining and Materials Engineering, Faculty of Engineering, Prince of Songkla University, Songkhla, Thailand

Nanocrystalline TiO₂ powder with and without Se doping were successfully synthesized at low temperature by a microwave-assisted sol-gel method. The synthesized TiO₂ powders were characterized by XRD, UV-vis, FT-IR and SEM. It was found that anatase and brookite phase was formed after refluxed at 80°C using a domestic microwave oven. The study also investigated the efficiency of this compound to inhibit the growth of Escherichia coli with various concentrations of 0, 0.5, 1.0 and 2.0 mole% doping Se. The antibacterial activity against Escherichia coli was investigated with a vitro test, from which the mixture of conidial suspension and the Se-doped TiO₂ powder was added to Macconkey Agar plates under fluorescent light irradiation. It was found that Se-doped TiO₂ nanoparticles enhance photocatalytic activity and bacterial inactivation efficiency. In addition, 1.0 mole %Se doped TiO₂ nanoparticles can destroy the bacteria within 10 min. Furthermore, the disinfection efficiency of Se-doped TiO₂ is good activity is mainly related to the high OH radicals on its surface. The absorption threshold of the Se-doped photocatalyst shifted to the visible region of the spectrum.

Keywords: Antibacterial activity, low temperature TiO₂ preparation, sol-gel.

1. Introduction

Human beings are continuously menaced by infection by microorganisms from contaminated air and water. Researchers have tried to develop effective antibacterial methods using various natural or inorganic materials [1]. Among them, titanium dioxide (TiO₂) has been intensively studied as a powerful antibacterial substance [2]. It has already been demonstrated that TiO₂ show strong oxidizing power through the generation of hydroxyl radicals (OH•) and superoxide anions (O₂^{•-}) under irradiation with UV light with a wavelength of less than 385 nm [3]. Although the exact bactericidal mechanism of these reactive oxygen species (ROS) is not clearly revealed, these ROS produced from photocatalytic activity of TiO₂ are extremely reactive with the microorganisms they come into contact with, and subsequently cells are killed or deactivated [4]. The photocatalytic activity of TiO₂ nanoparticles is mainly determined by its crystalline phase (anatase and rutile), crystallite size, specific surface area, pore structure, and crystallinity [5]. Many processes have been used for the deposition of TiO₂ films including sol-gel, hydrothermal synthesis followed by dip-coating, spray pyrolysis, pyrosol and chemical vapor deposition [6]. Nevertheless, these techniques generally require high preparing temperature to achieve the anatase phase formation; hence, they are inappropriate for polymer coating application.

Recently, there has been an evident of interest regarding the low temperature methods for fabrication of crystalline thin films of advanced materials such as semiconductors, from which not only from the point of view of energy saving, but also for the low thermally resistant substrates such as plastics, wood, or fibers have been reported [7]. Calcination at high temperatures is also incompatible with polymer substrates with poor thermal stability [8]. The anatase thin films based on the various polymeric substrates could be achieved by the deposition of the suspension of anatase particles, crystallized at low temperature or by the deposition of the titania gel following with the crystallization post-treatments by autoclaving or refluxing [9]. Various strategies have been pursued to modify TiO₂ such as metal ion doping [10–24], non-metal ion doping [22–30], surface modification [31,32] and doping with rare earth metals [33]. Transition metal ions like Fe³⁺, Cr³⁺, Co²⁺ and Mo²⁺ are usually employed to lower the band-gap and enhance the photocatalytic activity of TiO₂. The motivation of this study is in the published paper by Yelda et al. [34]. They have investigated the behavior of selenium (Se IV) ions by an incipient wet impregnation method into the bulk of TiO₂. And observed a red-shift in the absorption threshold of the resulting Se-mixed TiO₂ powders. Based on this result, we attempted to dope TiO₂ with selenium dioxide (SeO₂) to obtain an active, visible-light

* Autor corespondent/Corresponding author,
E-mail: susumeme1983@yahoo.com

driven photocatalyst and antibacterial activity. To the best of our knowledge, there is no study reported in the literature on Se-doped TiO₂. A recently published paper further strengthened our aim. Song et al. [35] have synthesized Se (II)-doped InOOH by a mild solvothermal method and concluded that Se(II)-doping narrows the band-gap of the photocatalyst.

In this work, nanocrystalline TiO₂ powder were synthesized at low temperatures by a microwave-assisted sol-gel method. The TiO₂ sol was prepared from titanium tetraisopropoxide (TTIP) in acidic aqueous solutions and was subsequently refluxed at 80°C for 2 h using a domestic microwave oven. The microstructural and the antibacterial behavior of synthesized powders were investigated.

2. Experimental Details

2.1. Preparation of Se Doped TiO₂ Nanoparticles

TiO₂ powders preparation Titanium (IV) isopropoxide (TTIP, 99.95%, Fluka Sigma-Aldrich) and selenium dioxide (SeO₂) were used as starting materials, while hydrochloric acid (Oriental Chemical Industries) was applied as a peptizer. It is noted that water used to prepare TiO₂ sols was distilled. The TiO₂ sol was synthesized by adding the mixture of TTIP (10 ml), ethanol (90 ml) (99.9%; Merck Germany) and SeO₂ (0, 0.5, 1.0 and 2.0 mol%) with water (125 ml) and stirring for 5 min at room temperature. Then 2 M hydrochloric acid was added drop wise to the solution adjust the pH of the system to 2. Then the solution was refluxed for 2 h by a domestic microwave oven at low working power (about 180 W) intermittently leading to a milky solution. The temperature of the solution was measured and controlled at 80°C. It was then dried in a domestic microwave oven at 100 W for 2 h until TiO₂ powders were formed. Finally, as received powders was ground using mortar in order to reduce the agglomerate grains. For Se-doped TiO₂ powder preparation was added in TiO₂ sols, while further processes were similar to those of pure TiO₂ preparation.

2.2. Material Characterizations

In order to determine the effect of Se doping on the crystal structure of TiO₂, X-ray diffraction (XRD) patterns were obtained (Phillips X'pert MPD, Cu-K). The band gap energy value of TiO₂ in the powder form was measured by UV-Vis-NIR Spectrometer with integrating sphere attachment (Shimadzu ISR-3100 spectrophotometer by using BaSO₄ as reference). The infrared spectra were recorded using Fourier-transformed infrared spectrophotometer (EQUINOX55, Bruker, Germany) in diffused reflectance mode at 4000–400 cm⁻¹ with KBr as blank. The morphological structure of the Se- doped TiO₂ photocatalysts was examined

on a Scanning Electron Microscope (SEM). The chemical composition of sample surface was investigated by X-ray photoelectron spectrometer (XPS; AXIS ULTRA^{DLD}, Kratos analytical, Manchester UK.) Spectrums were processed on software "VISION II" by Kratos analytical, Manchester UK. The base pressure in the XPS analysis chamber was about 5x10⁻⁹ torr. The samples were excited with X-ray hybrid mode 700x300 μm spot area with a monochromatic Al K_α 1,2 radiation at 1.4 keV. X-ray anode was run at 15kV 10 mA 150 W. The photoelectrons were detected with a hemispherical analyzer positioned at an angle of 45° with respect to the normal to the sample surface.

2.3. Antibacterial activity against *E. coli*

Escherichia coli (ATCC 25922) were used as a model bacterium to evaluate the antibacterial activity of TiO₂ nanoparticles. Antibacterial activity of synthesized powder against the bacteria *Escherichia coli* (*E. coli*) was studied and compared to the synthesized TiO₂ powder. Aliquots of 100 mL *E. coli* conidial suspension (10⁵ CFU/ml) were mixed with 50 mg of powder. The mixture was then exposed to visible light for 0, 5, 10, 15 and 20 min. Then, 0.1 mL of mixture suspension was sampled and spread on Macconkey Agar plate and incubated at 37°C for 24 h. After incubation, the number of viable colonies of *E. coli* on each Macconkey Agar plate was observed.

3. Results and discussion

3.1. Characterization of Se-Doped TiO₂ Nanoparticles and Preliminary Study

From the XRD study as shown in Fig. 1, the anatase peaks were observed at 25.50°, 37.59°, 48.01°, and 54.16°. A small broad signal at 30.64° is ascribed to TiO₂ brookite traces. It is commonly known that high calcination temperature, at least at 300°C, is required to achieve anatase TiO₂, while it can be successfully achieved here at a much lower temperature of 80°C. Furthermore, it can be seen that Se doping seems to hinder anatase crystal growth, especially at low temperature synthesis. These results confirm that Se-doped, can efficiently inhibit the anatase crystal growth. The spectrum (Fig. 2) for the undoped TiO₂ has a sharp absorption edge at around 380 nm, however, the absorption threshold of the doped TiO₂ shifted towards the visible region of the spectrum. In contrast to the undoped TiO₂, a high visible light absorption band from 420 nm extending up to 460 nm was obtained, which is consistent with the color of the samples. Thus, the utility range of light is widened, which in turn may considerably increase the photocatalytic activity of TiO₂ under visible light irradiation. From the UV-vis spectra shown in Table 1, the band gap energy of the 1.0mol % Se-doped TiO₂ is shifted by 0.52 eV compared to that of pure TiO₂ (3.20 eV).

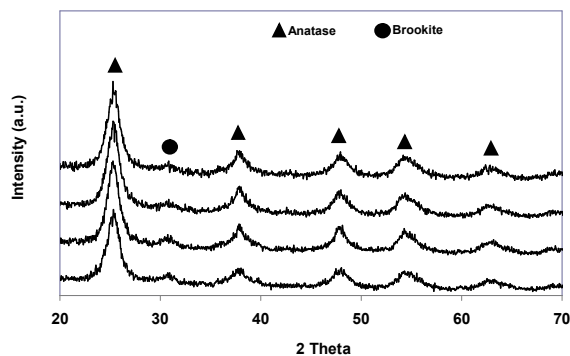


Fig.1 - XRD patterns of synthesized powders calcined at 100W using domestic microwave oven for 2 h for undoped and Se-doped TiO₂ powders.

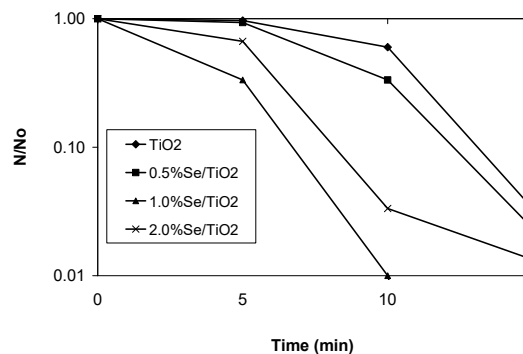


Fig. 3 - The survival rate of *E. coli* treated with synthesized powder exposed under fluorescent light irradiations compared with a TiO₂ powders.

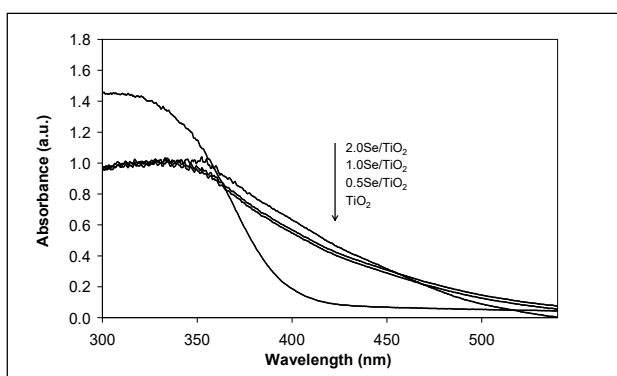


Fig.2 - UV-vis diffuse reflectance spectra of undoped TiO₂ and Se-doped TiO₂ samples

Table 1

Energy band gaps of Se-doped TiO ₂ powders	
Samples	Energy band gap (eV)
TiO ₂	3.20
0.5Se/TiO ₂	2.70
1.0Se/TiO ₂	2.68
2.0Se/TiO ₂	2.64

The band gap energy of 1.0mol % Se-doped TiO₂ was 2.68 eV. These shifts demonstrate show photocatalytic activity may be modulated by atomic-level doping of a nanocatalyst.

The absorption wavelength of the 1.0mol % Se-doped TiO₂ photocatalyst is extended toward visible light (=460 nm) relative to the other samples [34], giving it the highest photocatalytic activity. Fig. 3, show only 59% of bacteria were killed with synthesized pure TiO₂ powder. This is possibly due to the higher concentration of OH radicals which are very strong oxidant species against microbial on its surfaces. Antibacterial activity under fluorescent irradiations occurred at completely destroyed *E. coli* bacteria after 10 min. The further work could be studied on the development and simplify its use as a thin film coating. As shown in Fig. 4 present the number of bacteria survived after testing under fluorescent light showing the decrease in *E. coli* survivals with irradiation time. The result indicated that synthesized Se-doped TiO₂ exhibited higher

antibacterial activity compared to pure TiO₂ powder when exposed to fluorescent light.

The infrared spectra of synthesized titanium dioxide powders in the range 4000–400cm⁻¹ wave number are shown in Fig. 5. Photogenerated hydroxyl groups on the titanium dioxide surface were characterized using FTIR transmittance spectra mainly in the range of 3200–3600 cm⁻¹ [36]. The bands appearing at about 3400–3468 cm⁻¹ in Se-doped TiO₂ corresponded to stretching vibration of the OH groups linking with titanium atoms (TiO₂-OH) which arise from the hydrolysis reaction in the sol-gel process. The broad and strong peaks at 1630–1640 cm⁻¹ was ascribed to bending vibration of the OH group of free water or absorbed water [36]. These results confirmed the presence of hydroxyl group generated by the structure of the powders. The larger surface hydroxyl group density will lead to enhancement of the photocatalytic activity since they can interact with photogenerated holes, which give better charge transfer and inhibit the recombination of electron-hole pairs. The peak at approx.600 cm⁻¹ was ascribed to absorption bands of Ti-O and O- Ti-O flexion vibration. It can be seen that synthesized powder enhanced higher transmittance compared to TiO₂ powder due to the absence of high temperature calcination requirement.

The morphology of synthesized 1.0mol % Se-doped TiO₂ nanoparticles was studied using SEM. The nanoparticles were distributed uniformly with the formation of aggregated nanoparticles. It shows that the nanoparticles were densely dispersed with a narrow range of dispersion. Particles were of size with the smooth and rough surface (Fig. 6). The observed micrograph shows synthesized Se-doped TiO₂ aggregates and appears particles with the size less than 1 μm.

3.2. XPS analysis

Fig. 7 shows the X-ray photoelectron spectroscopic (XPS) survey spectra of TiO₂ and 1.0 mol% Se-doped TiO₂ thin films. The elements Ti, O, C and Se were clearly detected, and the

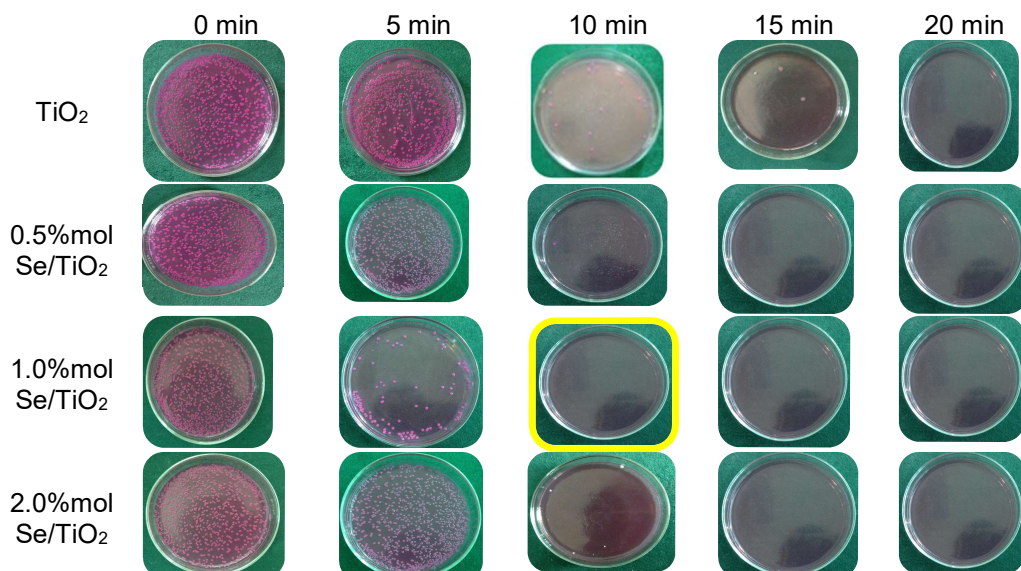


Fig. 4- Photo images for the results of *E. coli* test with synthesized powder under fluorescent light comparing with TiO₂ powder.

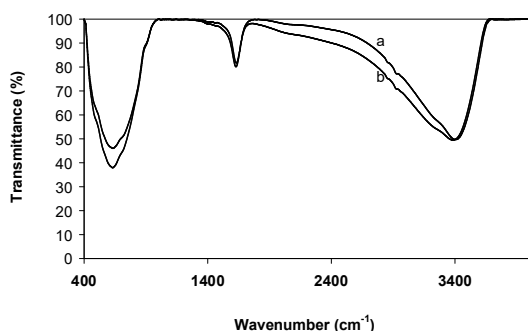


Fig. 5 - FTIR spectra of the synthesized (a) TiO₂ and (b) 1.0mol %Se-doped TiO₂ powders.

semiquantitative analysis estimated atomic fractions in this order were about 2.3, 26.4, 68.6 and 1.1 at%, for the 1.0 mol% Se-doped TiO₂ thin film. The XPS peaks indicate that the 1.0 mol% Se-doped TiO₂ thin films contain Ti, O, C and Se elements, and the binding energies of Ti2p, O1s, C1s and Se 3d are 458, 532, 285 and 59 eV, respectively.

The surface peak intensities of Ti reduced in the Se doped samples indicating the decrease in the surface Ti⁴⁺ content. The Ti 2p spectra of the Se-doped TiO₂ show the core binding energy (BE) levels at 458.7 eV for Ti 2p_{3/2} higher than 458.0 eV for the undoped TiO₂ (Fig. 8a and c). The higher binding energy indicates that the electronic interaction of Ti with selenium ions is different in the Se-doped TiO₂ from that in the undoped TiO₂. The binding energy of O 1s spectra in pure TiO₂ sample is 529.3 eV whereas in the Se-doped TiO₂ sample the binding energy of O 1s spectra 532.0 eV corresponding to the value of the one in the undoped TiO₂, which is assigned to the metallic oxide (O²⁻) in the TiO₂ lattice (Fig. 8b and d). This

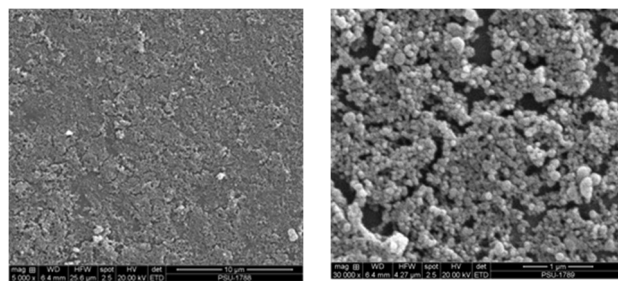


Fig. 6 - SEM images of synthesized 1.0 mol% Se-doped TiO₂ powders calcined at 100W using domestic microwave oven for 2 h at 5,000X (left) and 30,000X (right).

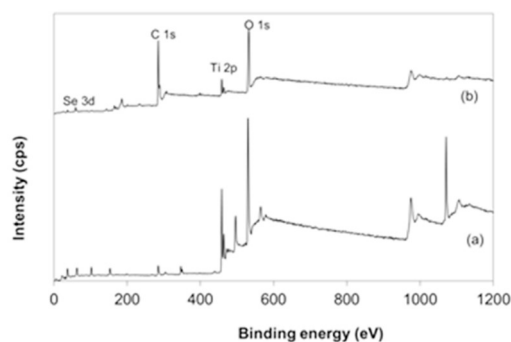


Fig. 7 - XPS spectra of a) TiO₂ and b) Se-doped TiO₂

may be attributed to the formation of the Ti–O–Se bonds in the crystal lattice. Since the electronegativity of Se is more than titanium, the electron density around titanium cations and oxygen anions decrease causing an increase in the binding energy [37]. In addition to an assess the state of selenium atoms in the Se-doped TiO₂ thin films, the signals of Se dopant were found to be weaker than all the others, due to the low doping

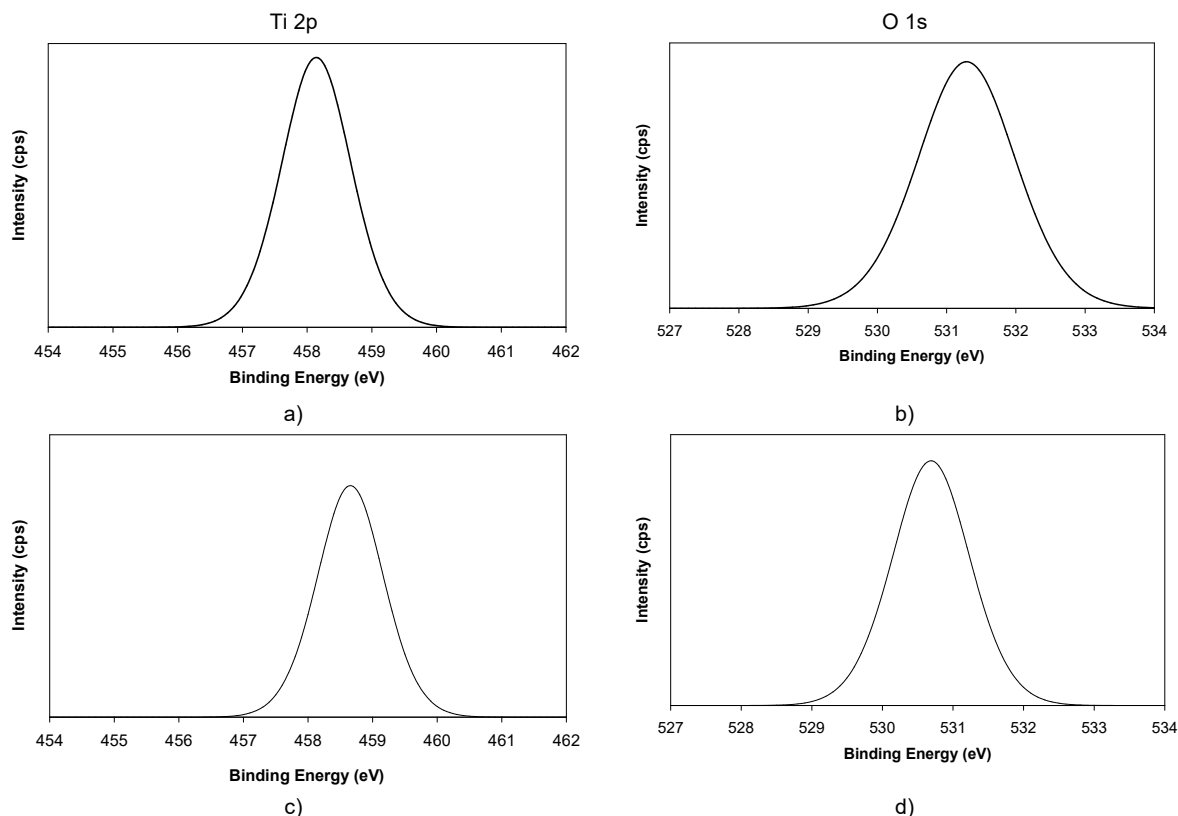


Fig. 8: XPS spectra of Ti 2p and O 1s of pure TiO₂ (a and b) and 1.0 mol %Se-doped TiO₂ (c and d).

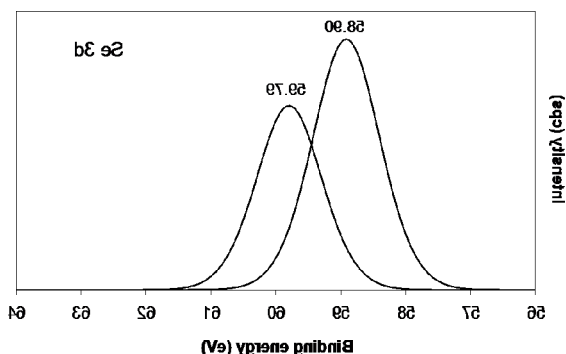


Fig. 9 - XPS spectrum of Se 3d on the surface of 1.0 mol% Se-doped TiO₂.

level. The Se 3d binding energy peaks were broad and asymmetric, indicating at least two chemical states of Se 3d lines (Se 3d 5/2 = 58.90 and 59.79 eV) as shown in Fig. 9. These peaks were the results of the introduction of the doping species during the synthesis process; the main peak at the binding energy of 58.90 and 59.79 eV was attributed to the selenium (IV) dioxide [37]. These observations reveal that selenium in the sample is in the form of Se (IV) that can penetrate into the TiO₂ lattice and substitute Ti⁴⁺ cations. The formation of the new Ti–O–Se bonds in the crystal lattice changes the electron densities of Ti⁴⁺ cations and O²⁻ anions causing a change in the charge distribution of the atoms on the photocatalyst surface which may enhance the photocatalytic

activity. The C element derived from the balances is other trace elements and the glass substrate.

4. Conclusion

Nanocrystalline TiO₂ powder with and without Se doping was successfully synthesized at low temperature by a microwave-assisted sol–gel method. It was found that Se-doped TiO₂ appear Se⁴⁺ from XPS data. The crystallization of TiO₂ precursor was obtained by refluxing using a domestic microwave oven. The fraction of Se was 1.0%mol showed excellent antibacterial activity against *E. coli*; it completely destroyed *E. coli* bacteria after 10 min with fluorescent light. It was also found that TiO₂ doped with Se powders to obtain a visible light active photocatalyst with high photocatalytic activity and the higher concentration of OH radicals which are very strong oxidant species against microbial than those of TiO₂ due to the absence of high temperature calcination requirement.

Acknowledgment

The research work was supported by the faculty of Engineering Rajamangala University of Technology Srivijaya, Songkhla, Thailand. We would like also to acknowledge the Materials Engineering Research Center (MERC), Faculty of Engineering, Prince of Songkla University for their facility supports.

REFERENCES

1. T.N. Kim, Q.L. Feng, J.O. Kim, J. Wu, H. Wang, G.C. Chen, F.Z. Cui, Antimicrobial effects of metal ions (Ag⁺, Cu²⁺, Zn²⁺) in hydroxyapatite, *Journal of Materials Science: Materials in Medicine*, 1998, **9**(3), 129.
2. P. Maness, S. Smolinski, D.M. Blake, Z. Huang, E.J. Wolfrum, W.A. Jacoby, Bactericidal activity of photocatalytic TiO₂ reaction: toward an understanding of its killing mechanism, *Applied and Environmental Microbiology*, 1999, **65**(9), 4094.
3. P.A. Christensen, T.P. Curtis, T.A. Egerton, S.A.M. Kosa, J.R. Tinlin, Photoelectrocatalytic and photocatalytic disinfection of *E. coli* suspensions by titanium dioxide, *Applied Catalysis, B: Environmental*, 2012, **41**(4), 371.
4. K. Sunada, T. Watanabe, K. Hashimoto, Studies on photokilling of bacteria on TiO₂ thin film, *Journal of Photochemistry and Photobiology, A: Chemistry*, 2003, **156**, 227.
5. S.M. Chin, E.S. Park, M.S. Kim, J.S. Jung, Photocatalytic degradation of methylene blue with TiO₂ nanoparticles prepared by a thermal decomposition process, *Powder Technology*, 2010, **201**(2), 171.
6. F.D. Duminica, F. Maury, R. Hausbrand, Growth of TiO₂ thin films by AP-MOCVD on stainless steel substrates for photocatalytic applications, *Surface and Coatings Technology*, 2007, **201**(22–23), 9304.
7. L. Ge, M. Xu, M. Sun, H. Fang, Fabrication and characterization of nano TiO₂ thin films at low temperature, *Materials Research Bulletin*, 2006, **41**(9), 1596–1603.
8. Y.J. Yun, J.S. Chung, S. Kim, S.H. Hahn, E.J. Kim, Low-temperature coating of sol-gel anatase thin films, *Materials Letters*, 2004, **58**(29), 3703.
9. Z. Liuxue, W. Xiulian, L. Peng, S. Zhixing, Low temperature deposition of TiO₂ thin films on polyvinyl alcohol fibers with photocatalytic and antibacterial activities, *Applied Surface Science*, 2008, **254**(6), 1771.
10. T. Bala, G. Armstrong, F. Laffir, R. Thornton, Titania–silver and alumina–silver composite nanoparticles: novel, versatile synthesis, reaction mechanism and potential antimicrobial application, *Journal of colloid and interface science*, 2011, **356**(2), 395.
11. S. Boonyod, W. Suttisripok, L. Sikong, Antibacterial activity of TiO₂ and Fe³⁺ doped TiO₂ nanoparticles synthesized at low temperature, *Advanced Materials Research*, 2011, **214**, 197.
12. W. Choi, A. Termin, M. R. Hoffmann, The role of metal ion dopants in quantum-sized TiO₂: correlation between photoreactivity and charge carrier recombination dynamics, *Journal of physical chemistry*, 1994, **98**(51), 13669.
13. K. Nagaveni, M.S. Hegde, G. Madras, Structure and photocatalytic activity of Ti_{1-x}M_xO_{2+δ} (M = W, V, Ce, Zr, Fe and Cu) synthesized by solution combustion method, *The Journal of Physical Chemistry B*, 2004, **108**(52), 20204.
14. A. Di Paola, G. Marci, L. Palmisano, M. Schiavello, K. Uosaki, S. Ikeda, B. Ohtani, Preparation of polycrystalline TiO₂ photocatalysts impregnated with various transition metal ions: characterization and photocatalytic activity for the degradation of 4-nitrophenol, *The Journal of Physical Chemistry B*, 2002, **106**(3), 637.
15. W. Mu, J.M. Hermann, P. Pichat, Room temperature photocatalytic oxidation of liquid cyclohexane into cyclohexanone over neat and modified TiO₂, *Catalysis Letters*, 1989, **3**(1), 73.
16. K.E. Karakitsou, X.E. Verykios, Effects of intervalent cation doping of TiO₂ on its performance as a photocatalyst for water cleavage, *ChemInform*, 1993, **97**(6), 1184.
17. P. Bouras, E. Stathatos, P. Lianos, Pure versus metal-ion-doped nanocrystalline titania for photocatalysis, *Applied Catalysis B: Environmental*, 2007, **73**(1), 51.
18. Y. Wu, J. Zhang, L. Xiao, F. Chen, Preparation and characterization of TiO₂ photocatalysts by Fe³⁺ doping together with Au deposition for the degradation of organic pollutants, *Applied Catalysis B: Environmental*, 2009, **88**(3), 525.
19. A. Fuerte, M.D. Hernández-Alonso, A.J. Maira, A. Martínez-Arias, M. Fernández-García, J.C. Conesa, J. Soria, Visible light-activated nanosized doped-TiO₂ photocatalysts, *Chemical Communications*, 2001, (24), 2718.
20. L.G. Devi, S.G. Kumar, Influence of physicochemical–electronic properties of transition metal ion doped polycrystalline titania on the photocatalytic degradation of Indigo Carmine and 4-nitrophenol under UV/solar light, *Applied Surface Science*, 2011, **257**(7), 2779.
21. S. Buddee, S. Wongnawa, U. Sirimahachai, W. Puetpaibool, Recyclable UV and visible light photocatalytically active amorphous TiO₂ doped with M (III) ions (M = Cr and Fe), *Materials Chemistry and physics*, 2011, **126**(1), 167.
22. C.Y. Wang, C. Böttcher, D.W. Bahnemann, J.K. Dohrmann, A comparative study of nanometer sized Fe (III)-doped TiO₂ photocatalysts: synthesis, characterization and activity, *Journal of Materials Chemistry*, 2003, **13**(9), 2322.
23. M.A. Khan, S.I. Woo, O.B. Yang, Hydrothermally stabilized Fe (III) doped titania active under visible light for water splitting reaction, *International Journal of Hydrogen Energy*, 2008, **33**(20), 5345.
24. S. Songara, M.K. Patra, M. Manoth, L. Saini, V. Gupta, G.S. Gowd, S.R. Vadera, N. Kumar, Synthesis and studies on photochromic properties of vanadium doped TiO₂ nanoparticles, *Journal of Photochemistry and Photobiology A: Chemistry*, 2010, **209**(1), 68.
25. T.C. Jagdale, S.P. Takale, R.S. Sonawane, H.M. Joshi, S.I. Patil, B.B. Kale, S.B. Ogale, N-doped TiO₂ nanoparticle based visible light photocatalyst by modified peroxide sol-gel method, *The Journal of Physical Chemistry C*, 2008, **112**(37), 14595.
26. S. Sakthivel, H. Kisch, Daylight photocatalysis by carbon-modified titanium dioxide, *Angewandte Chemie International Edition*, 2003, **42**(40), 4908.
27. T. Ohno, M. Akiyoshi, T. Umebayashi, K. Asai, T. Mitsui, M. Matsumura, Preparation of S-doped TiO₂ photocatalysts and their photocatalytic activities under visible light, *Applied Catalysis A: General*, 2004, **265**(1), 115.
28. R. Zheng, L. Lin, J. Xie, Y. Xie, State of doped phosphorus and its influence on the physicochemical and photocatalytic properties of P-doped titania, *The Journal of Physical Chemistry C*, 2008, **112**(39), 15502.
29. N. Lu, H. Zhao, J. Li, X. Quan, S. Chen, Characterization of boron-doped TiO₂ nanotube arrays prepared by electrochemical method and its visible light activity, *Separation and Purification Technology*, 2008, **62**(3), 668.
30. Y.W. Sakai, K. Obata, K. Hashimoto, H. Irie, Enhancement of visible light-induced hydrophilicity on nitrogen and sulfur-codoped TiO₂ thin films, *Vacuum*, 2008, **83**(3), 683.
31. S.H. Bossmann, S. Göb, T. Siegenthaler, A. M. Braun, K.T. Ranjit, I. Willner, An N, N'-dialkyl-4, 4'-bipyridinium-modified titanium-dioxide photocatalyst for water remediation-observation and application of supramolecular effects in photocatalytic degradation of p-donor organic compounds, *Fresenius' journal of analytical chemistry*, 2001, **371**(5), 621.
32. E.H. Mert, Y. Yalçın, M. Kılıç, N. San, Z. Çınar, Surface modification of TiO₂ with ascorbic acid for heterogeneous photocatalysis: theory and experiment, *Journal of Advanced Oxidation Technologies*, 2008, **11**(2), 199.
33. M. Bellardita, A. Di Paola, L. Palmisano, F. Parrino, G. Buscarino, R. Amadelli, Preparation and photoactivity of samarium loaded anatase, brookite and rutile catalysts, *Applied Catalysis B: Environmental*, 2011, **104**(3), 291.
34. Y.Y. Gurkan, E. Kasapbasi, Z. Cinar, Enhanced solar photocatalytic activity of TiO₂ by selenium (IV) ion-doping: characterization and DFT modeling of the surface, *Chemical engineering journal*, 2013, **214**, 34.
35. L. Song, C. Chen, S. Zhang, Q. Wei, Synthesis of Se-doped InOOH as efficient visible-light-active photocatalysts, *Catalysis Communications*, 2011, **12**(11), 1051.
36. K. Lv, H. Zuo, J. Sun, K. Deng, S. Liu, X. Li, D. Wang, (Bi,C and N) codoped TiO₂ nanoparticles, *Journal of Hazardous Materials*, 2009, **161**(1), 396.
37. Y.G. Yelda, K. Esra, C. Zekiye, Enhanced solar photocatalytic activity of TiO₂ by selenium (IV) ion-doping: characterization and DFT modeling of the surface, *Chemical Engineering Journal*, 2013, **214**, 34.
